JOURNAL OF CATALYSIS 130, 528–546 (1991)

Divergent Pathways of Acetaldehyde and Ethanol Decarbonylation on the Rh(111) Surface

C. J. HOUTMAN AND M. A. BARTEAU

Center for Catalytic Science and Technology, University of Delaware, Newark, Delaware 19716

Received November 30, 1990; revised March 25, 1991

The decomposition reactions of acetaldehyde and ethanol on the Rh(111) surface were compared in temperature-programmed desorption (TPD) and high-resolution electron energy loss spectroscopy (HREELS) experiments. The decarbonylation of acetaldehyde produced methane at 267 K in TPD. The selectivity to methane was dependent on the initial coverage of acetaldehyde. For acetaldehyde coverages less than 0.05 monolayer, no methane was desorbed, but for a coverage that saturated the first layer, methane was produced with 50% selectivity. Coadsorbing deuterium with a low coverage of acetaldehyde resulted in the enhancement of methane production. This result indicates that the selectivity to methane was partially controlled by the availability of hydrogen atoms on the surface required to hydrogenate the hydrocarbon species produced by acetaldehyde decarbonylation. Monodeuterated methane was the primary methane product observed after these coadsorption experiments. Thus it was concluded that acetaldehyde decarbonylates via a methyl migration mechanism on the Rh(111) surface. Decarbonylation of ethanol did not produce methane. The absence of methane production indicated that the decomposition of ethanol on the Rh(111) surface did not proceed via dehydrogenation to adsorbed acetaldehyde, but instead, ethanol appeared to dehydrogenate by methyl hydrogen abstraction resulting in the formation of an oxametallacycle. Since this proposed intermediate rapidly dehydrogenated to carbon monoxide and surface carbon, it was difficult to characterize spectroscopically. The existence of an ethanol decomposition pathway that does not include acetaldehyde intermediates indicates that ethanol formation on supported Rh catalysts may not be the result of acetaldehyde hydrogenation. Support for ethanol synthesis pathways that both do and do not include acetaldehyde can be found in previous studies of ethanol formation on supported Rh catalysts. This surface science study has allowed the identification of some of the factors that may control the selectivity of higher oxygenate decomposition/synthesis pathways.

INTRODUCTION

Ethanol and acetaldehyde formation from CO and H_2 on supported rhodium catalysts has been the subject of several studies. Takeuchi and Katzer (*1*) suggested that CO insertion into methylene moieties on the surface was the pivotal step in ethanol formation on Rh/TiO_2 catalysts. They proposed the formation of a surface ketene species on the basis of isotopic scrambling of labeled CO during ethanol formation. Their proposed mechanism provided a pathway to ethanol that did not include acetaldehyde intermediates but proceeded via adsorbed vinyl alcohol and ethylene oxide species. The method of isotopic labelling was also used by Orita *et al.* (*2*) to support the conclusion that ethanol was not the product of acetaldehyde hydrogenation in syngas reactions on Rh/SiO_2. They suggested that the formation of carboxylate species on the support played a role in the formation of ethanol. A Rh/SiO_2 catalyst was studied by Jackson *et al.* (*3*) who also showed that ethanol was not the product of acetaldehyde hydrogenation in the CO plus H_2 reaction. This conclusion was based on the observation that ethanol and acetaldehyde exhibited different extents of isotopic incorporation from labeled carbon monoxide. They proposed that acetaldehyde was formed via an acetyl intermediate, while ethanol was formed via an alkoxide-like intermediate that was

0021-9517/91 $3.00

bonded through both the oxygen and the methyl carbon, forming an oxametallacycle. In contrast, Underwood and Bell recently concluded that acetaldehyde was indeed hydrogenated to ethanol by supported rhodium catalysts in the syngas reaction (*4*). This conclusion was based on two sets of experiments. They showed that ethanol production was favored over acetaldehyde by longer residence times, indicative of a sequential reaction leading to ethanol via an acetaldehyde intermediate. They also demonstrated that adding acetaldehyde to the feed stream enhanced the production of ethanol. The evidence for acetaldehyde hydrogenation was most dramatic for Rh on La_2O_3 catalysts, but some hydrogenation was also indicated for SiO_2-supported catalysts.

There have been a number of mechanisms proposed for ethanol and acetaldehyde production on supported rhodium catalysts which include intermediates such as ketenes, carboxylates, alkoxides and aldehydes. The role of the support in determining the reaction pathways is unclear. The selectivity of rhodium catalysts used for CO hydrogenation has proven to be quite sensitive to the identity of the support/promoter. This sensitivity was first shown by Ichikawa (*5*). He reported that rhodium supported on ZrO_2, TiO_2, or La_2O_3 produced primarily ethanol; rhodium on MgO or ZnO produced methanol; and rhodium on SiO_2 or Al_2O_3 produced primarily methane. Lavalley *et al.* (*6*) have recently summarized the current theories regarding promoter/support effects. These theories include stabilization of rhodium in a higher oxidation state by the support, the activation of the CO molecule at the metal-support interface, and the stabilization of oxygenated intermediates on the support. Since the reactions and relevant intermediates on the metal surface are not known, the participation of the support in this chemistry is difficult to determine. A first step in developing a clearer understanding of supported rhodium catalysts is to identify the stable intermediates formed from acetaldehyde and ethanol on the metal surface. The mechanism of ethanol and acetaldehyde decomposition on the Rh(111) surface was the focus of the present work. By examining the chemistry of these molecules without the complexity caused by support and promoter effects, the role of the metal in the catalytic synthesis of these higher oxygenates may become more clear.

Acetaldehyde decomposition has been examined previously on the Ru(0001) and Pd(111) surfaces under ultrahigh vacuum conditions. Henderson *et al.* (*7*) found that acetaldehyde bound in an η^2(C,O) configuration decomposed on Ru(0001) at 315 K in TPD experiments. This decomposition resulted in the desorption of hydrogen, the production of carbon monoxide, and the deposition of surface hydrocarbon fragments. These workers also suggested that the polymerization of acetaldehyde occurred both on the surface and in the multilayer of molecules adsorbed on top of the first layer. Davis and Barteau (*8*) observed the dehydrogenation of acetaldehyde to acetyl intermediates on the Pd(111) surface. The acetyl was characterized by a ν(CO) frequency of 1565 cm^{-1}. They also identified an η^2(C,O)-acetaldehyde intermediate. This species had a ν(CO) frequency at 1390 cm^{-1} which indicated that the η^2(C,O)-bonding configuration resulted in a significant reduction in the carbonyl bond order. Hydrogen, methane, carbon monoxide, and surface carbon were produced from the decomposition of acetaldehyde on the Pd(111) surface. Comparison of the decomposition temperatures of acetyl and deuterated acetyl species showed a kinetic isotope effect (KIE). This KIE indicated that C–H bond cleavage at the methyl group preceded the C–C bond cleavage. Approximately 90% of the methylene groups formed via this route were hydrogenated to methane, and 10% were dehydrogenated to surface carbon. The methane was evolved in a reaction-limited desorption peak at 375 K. Davis and Barteau also examined ethanol decomposition on the Pd(111) surface by TPD (*9*) and HREELS (*10*). Ethoxide was formed upon adsorption at 170 K. The dehy-

drogenation of ethoxide produced adsorbed acetaldehyde at 200 K; above this temperature the reactions of adsorbed layers derived from ethanol and acetaldehyde on Pd(111) were very similar in all respects. A similar decomposition sequence for ethanol on the Ni(111) surface has been reported by Gates *et al.* (*11*) based on experiments with various isotopically labeled reactants. The first step was ethoxide formation followed by C–H bond cleavage at the methylene carbon. From this point in the decomposition sequence either acetaldehyde was desorbed from the surface or the C–C bond was cleaved, presumably releasing a methyl group that was subsequently hydrogenated to methane. The elimination of methyl groups from the aldehyde intermediate was suggested as the primary pathway by the isotopic distribution of the methane evolved from selectively deuterated ethanol; however, the isotopic distributions did not contain only the expected product. Methane molecules that exchanged more than one hydrogen or deuterium atom were also observed. Gates *et al.* (*11*) explained the products exhibiting multiple isotopic substitution as the result of scrambling of hydrogen atoms between the surface and the methyl groups adsorbed on it; however, their isotopic distributions could also indicate that C–H cleavage on the methyl group could precede C–C bond cleavage as observed for acetaldehyde decomposition on Pd (*8*).

With several questions about the mechanism of ethanol and acetaldehyde formation arising from the results of studies on supported catalysts and a substantial amount of work with ethanol and acetaldehyde on other single-crystal surfaces for comparison, the study of these two molecules on the Rh(111) surface provides information about the role of the unsupported, unpromoted metal. In this work TPD was used to determine the selectivity to various products and to estimate the energetics of the processes observed. HREELS was used to identify the intermediates responsible for the reactions observed in TPD. These results demonstrate a surprising divergence of pathways for acetaldehyde and ethanol decomposition on the Rh(111) surface.

EXPERIMENTAL

Experiments were carried out in an ion- and diffusion-pumped vacuum chamber previously described (*12*). This instrument was equipped with a HREEL spectrometer (McAllister Technical Services), four grid optics (Physical Electronics) for AES and LEED, and a quadrupole mass spectrometer (UTI 100C) multiplexed with an IBM XT. The mass spectrometer ionizer was enclosed by a quartz shroud with a 7-mm hole at the entrance and two side vents. This shroud enhanced the collection of products in TPD experiments and minimized the sensitivity to species desorbed from the crystal support hardware.

The polished, (111)-oriented Rh single crystal was spot welded onto two 0.5-mm tantalum wires that served as supports as well as heating elements when a current was supplied. The crystal was cooled to ca. 85–90 K by thermal conduction through a 0.25-in. copper feedthrough, the opposite side of which was immersed in liquid nitrogen. The temperature of the Rh(111) sample was monitored with a chromel–alumel thermocouple spot welded to the back. The sample was cleaned by cycles of ion bombardment, oxygen TPD, and annealing to 1400 K. The surface produced by this treatment was determined to be clean using AES, HREELS, and oxygen TPD. The last of these was sufficient to detect (and remove) surface carbon to below the level of 0.005 monolayers.

The acetaldehyde and ethanol samples were stored in separate glass tubes attached to a stainless-steel manifold by all-metal valves. These samples were purified by repeated freeze/pump/thaw cycles, and were dosed onto the crystal through a 1.5-mm stainless-steel needle attached to the dosing line. Following the adsorption of reactants and recovery of the chamber background pressure, either TPD or HREELS experi-

ments could be carried out. In TPD experiments the sample temperature was ramped linearly (4.0 ± 0.2 K s^{-1}) under computer control, and up to eight mass fragments of the desorbing products were monitored with the multiplexed mass spectrometer. In HREELS experiments energy loss spectra were typically obtained for specular reflection of a 5 eV electron beam from the surface. The typical height and width of the elastically scattered beam were 6.5×10^5 counts per second at a FWHM of 70 cm^{-1}. Temperature-programmed steps between HREELS experiments were also carried out at 4 K s^{-1}. When the desired temperature had been reached the power supply was turned off and the crystal was allowed to cool to the initial temperature before collection of each HREEL spectrum.

RESULTS

Acetaldehyde on the Rh(111) Surface

Acetaldehyde underwent decarbonylation on the Rh(111) surface. Figure 1 shows the TPD spectrum following the adsorption of 1.5 Langmuirs (L) of acetaldehyde at 90 K. Hydrogen desorption from an initially clean surface with an equivalent hydrogen atom coverage exhibits a peak at 267 K. Since the peak maximum of the hydrogen desorption observed for acetaldehyde decomposition was 295 K, the leading edge of this peak was limited by the kinetics of the hydrogen-producing reaction, and the remainder of the peak followed the second-order kinetics of the formation of dihydrogen from atomic hydrogen. The second hydrogen desorption peak, at 390 K, was clearly reaction limited. Similar hydrogen desorption peaks were observed after the adsorption of hydrocarbons on the Rh(111) surface (*13*); the reaction resulting in the higher-temperature hydrogen peak was, therefore, assigned to the dehydrogenation of surface hydrocarbon species. The area under this peak represented a yield of 0.033 ML of hydrogen molecules. One monolayer (ML) is defined as the number of surface Rh atoms on the (111) surface, 1.62×10^{15} atoms /cm^2. Since the total H_2 yield was 0.16 ML, 21% of the hydrogen desorbed in the higher-temperature peak. The amount of carbon left on the surface after the TPD experiment was 0.091 ML. This was determined from a subsequent TPD experiment by integrating the CO and CO_2 desorption peaks observed following the adsorption of 1.2 L of oxygen. The yield of H_2 at 390 K and the $C_{(ad)}$ coverage indicated that the stoichiometry of the surface hydrocarbon moiety was approximately CH. Parallel with the pathway that resulted in the deposition of carbon and the desorption of hydrogen was a pathway leading to the formation of methane. Since methane does not adsorb on transition metals above 150 K (*14*), the methane peak at 267 K was clearly reaction limited. This peak represented 0.083 ML of methane. Thus, after the dose shown in Fig.

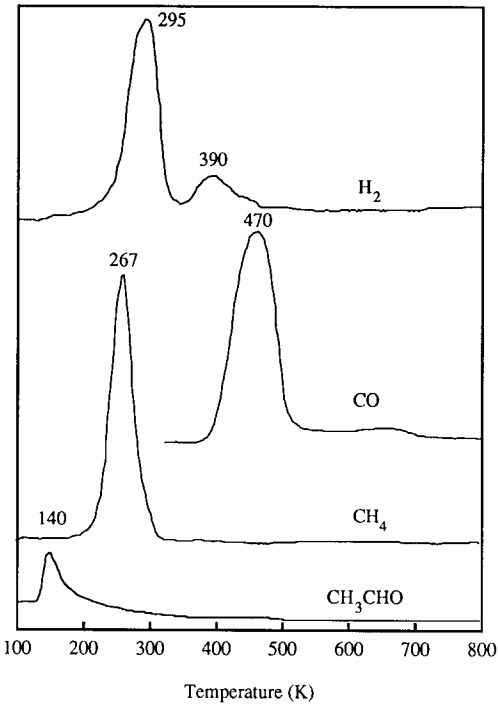

FIG. 1. TPD after an exposure of 1.5 L of acetaldehyde at 90 K. Yields corresponding to this spectrum were 0.16 ML of hydrogen, 0.08 ML of methane, 0.09 ML of surface carbon, 0.17 ML of carbon monoxide, and 0.12 ML of acetaldehyde.

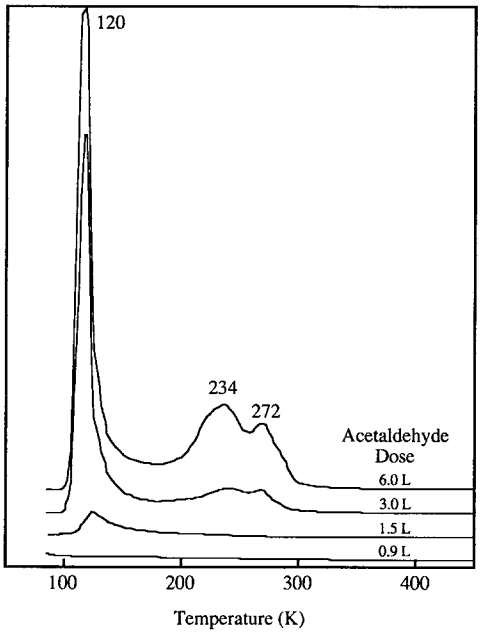

FIG. 2. TPD of acetaldehyde after the indicated exposures of acetaldehyde at 90 K. The amounts of acetaldehyde desorbed which corresponded to these spectra were 1.84 ML for 6.0 L, 0.97 ML for 3.0 L, 0.12 ML for 1.5 L, and <0.02 ML for 0.9 L.

1, approximately 50% of the methyl carbons of the parent acetaldehyde left the surface as methane and 50% were deposited as atomic carbon. The CO peak at 470 K was consistent with the desorption of molecular CO from the Rh(111) surface. The amount of CO represented by this peak was 0.17 ML. Since the sum of the amounts of surface carbon deposited and methane desorbed was 0.174 ML, the amount of CO desorbed was consistent with the stoichiometry of acetaldehyde. Finally, 0.12 ML of acetaldehyde desorbed at 140 K. The low temperature of this peak was indicative of a physically adsorbed state; the corresponding activation energy for desorption, obtained using the method of Redhead (*15*), was 35 kJ/mole, assuming a preexponential factor of 10^{13} s^{-1}. The assignment of this peak to a condensed state was confirmed by exposure of the surface to larger amounts of acetaldehyde. In Fig. 2 the acetaldehyde desorption peaks observed after various exposures of acetaldehyde are shown. The 140 K peak increased in intensity and decreased in temperature to 120 K with higher exposures (>1.5 L). This figure also shows the development of an additional pair of desorption states for acetaldehyde at higher exposures. After a 6-L exposure of acetaldehyde, 41% of the acetaldehyde desorbed via these channels at 234 and 272 K. The total acetaldehyde desorbed after a 6.0-L exposure was equivalent to 1.84 ML or approximately nine times the amount of CO desorbed during the same experiment. The acetaldehyde desorption peaks at 234 and 272 K were very similar to those observed by Henderson *et al.* (*7*) for high coverages of acetaldehyde on Ru(0001). They attributed acetaldehyde peaks at 250 and 310 K to the depolymerization of an acetaldehyde polymer. This polymer was suggested to be a physically adsorbed overlayer rather than the result of a reaction at the metal surface. Since the higher-temperature acetaldehyde desorption peaks were only observed after the multilayer state began to fill, polymerization in the overlayer and not on the surface was a likely explanation.

The coverage dependence of the product yields during acetaldehyde TPD is illustrated in Fig. 3. The yields of hydrogen,

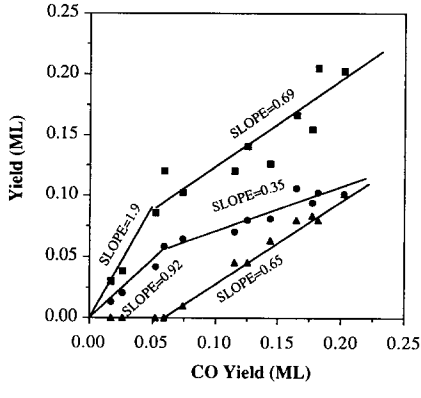

FIG. 3. TPD yields after acetaldehyde exposures (■H_2, ▲CH_4, ● surface carbon) plotted versus the yield of CO. The axes have units of monolayers.

methane, and surface carbon are plotted versus CO yield. Two selectivity regimes are apparent in this figure. For CO yields below 0.06 ML, the slope of the hydrogen yield line (i.e., the H_2/CO ratio) was 1.9 and that of the surface carbon yield line was 0.92, thus stoichiometric decarbonylation of acetaldehyde and the subsequent dehydrogenation of the resulting hydrocarbon moieties accounted for essentially the entire product slate. The evolution of methane was first observed for a CO yield of 0.06 ML. Since methane production provided an alternative to carbon deposition, the slopes of the hydrogen and carbon yield lines dropped. For the higher coverage regime the stoichiometry of acetaldehyde was still preserved among the products. The sum of the slopes of the methane yield line and the surface carbon yield line was 1.0, and the slope of the hydrogen line was twice that of the carbon yield line. For acetaldehyde exposures of 1.5 L and above the extent of decomposition of acetaldehyde saturated. The maximum amount of acetaldehyde that decomposed on the clean surface was 0.21 ML. Doses higher than 1.5 L resulted in larger amounts of acetaldehyde desorbed in TPD, as illustrated by Fig. 2, but no additional decomposition occurred. Since acetaldehyde desorption was not observed for doses lower than 1.0 L, the first monolayer appeared to decompose completely, and higher exposures of acetaldehyde resulted in adsorption on top of this reactive layer.

Acetaldehyde was coadsorbed with deuterium atoms in order to identify the origin of the two decomposition regimes and to determine the influence of the hydrogen coverage on the hydrocarbon yield from decarbonylation. Figure 4 illustrates the TPD spectra obtained after two experiments. One set of spectra was obtained after exposing a surface that contained 0.40 ML of preadsorbed deuterium atoms (generated by a 1.2-L exposure to D_2) to 0.2 L of acetaldehyde, and the other was the TPD after the clean Rh(111) surface was exposed to 0.2 L of acetaldehyde. The yields for these experiments are summarized in Table 1. For the case without excess deuterium atoms, 96% of the adsorbed acetaldehyde decomposed to hydrogen, carbon monoxide, and surface carbon; in the presence of $D_{(ad)}$ only 70% of the acetaldehyde decomposed completely. The remaining 30% of the methyl carbons reacted to form methane. The enhancement of the methane production with the addition of deuterium atoms indicated that the boundary between the two decomposition regimes identified in Fig. 3 could be shifted by increasing the hydrogen availability. Ap-

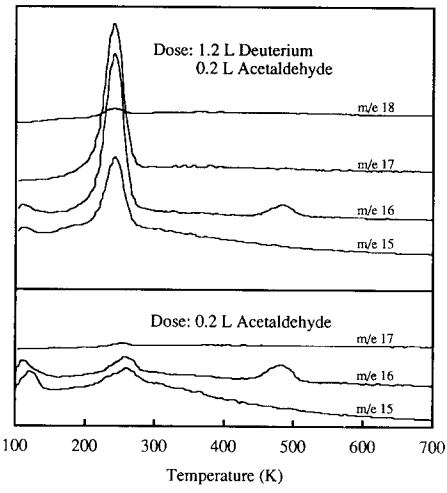

FIG. 4. Comparison of the TPD after an exposure of 1.2 L of deuterium and 0.2 L of acetaldehyde with the TPD after an exposure of 0.2 L of acetaldehyde. The yields for these spectra are summarized in Table 1.

TABLE 1

Acetaldehyde/Deuterium Codose TPD Yields (Monolayers)

Deuterium dose (L)	0.00	1.20
Acetaldehyde dose (L)	0.20	0.20
H_2 Yield	0.13	0.021
HD Yield	—	0.14
D_2 Yield	—	0.21
CH_4 Yield	0.0016	0.0039
CH_3D Yield	—	0.0081
CH_2D_2 Yield	—	0.0003
CO Yield	0.062	0.051

parently at low acetaldehyde coverages the hydrocarbon moieties released by decarbonylation dehydrogenated completely before they could react with the adsorbed hydrogen atoms. At higher acetaldehyde coverages, however, there were more hydrogen atoms available for reaction with the hydrocarbon. The availability of hydrogen atoms did not appear to be the only factor controlling the decomposition. Even with a deuterium atom to acetaldehyde ratio of 12 : 1, 70% of the 0.051 ML of hydrocarbon groups eliminated by acetaldehyde decarbonylation still dehydrogenated completely to surface carbon.

The identity of the hydrocarbon species released by the decarbonylation of acetaldehyde was also determined from the deuterium/acetaldehyde codose experiments. The desorption of monodeuterated methane (*m/e* 17) accompanied by insignificant amounts of multiply deuterated methane species indicated that the decarbonylation of acetaldehyde released methyl groups to the surface. Analysis of the methane desorption peak areas from the coadsorption experiment showed that 68% of the methane was CH_3D, 30% was CD_4, and only 2% contained multiple deuterium atoms. Analysis of the hydrogen/deuterium desorption peaks (*m/e* 2, 3, and 4) observed during this experiment showed that 76% of the atoms available for reaction with the methyl groups were deuterium. Thus the amount of deuterium scavenged by methyl groups to form methane essentially reflected the hydrogen to deuterium atomic ratio on the surface during the decarbonylation reaction.

Similar TPD experiments were also conducted with acetaldehyde-d_4 to test for a kinetic isotope effect. The peak temperature for methane-d_4 from acetaldehyde-d_4 was only 2 K higher than the methane peak temperature observed after acetaldehyde adsorption. This temperature difference implies a k_H/k_D ratio of 1.2 at 300 K; however, the uncertainty in the temperature measurement was approximately the same magnitude. Thus deuteration of the acetaldehyde did not produce a primary kinetic isotope effect on decarbonylation rate, and C—C bond scission is likely the rate-determining step in decarbonylation. Provided that the adsorbed species is CH_3CHO or CH_3CO this observation is consistent with the conclusion above that methyl groups are eliminated intact. These observations were in sharp contrast to those for other carbonyl compounds on Rh and Pd surfaces. On Pd(111) acetaldehyde formed stable acetyls ($CH_3C{=}O$); the decarbonylation of these species exhibited a primary kinetic isotope effect, suggesting that C—H scission preceded C—C scission (*8*). The rate-determining step in acetone decarbonylation on Rh(111) is C—H scission, since k_H/k_D ratios of 7 to 9 were observed for this reaction (*16*). The difference in the methane yields from acetaldehyde and acetone on Rh(111) was also consistent with the difference in the sequence of bond breaking for these two reactants deduced from measurements of the kinetic isotope effect. The rate-determining scission of C—H bonds prior to CO elimination suggests that methyl groups were not released intact by acetone decarbonylation, and only trace amounts of methane were produced from this reaction. Acetaldehyde decarbonylation releases methyl groups intact, and significant methane yields were observed.

In summary, the TPD experiments showed that the first monolayer of acetaldehyde adsorbed on the clean Rh(111) surface decarbonylated to release methyl groups to the surface at 267 K. The methyl groups were observed to undergo either hydrogenation to form methane or dehydrogenation which ultimately resulted in the deposition of surface carbon. Polymerization of the acetaldehyde overlayer was observed after exposures greater than 2.0 L.

HREELS was used to identify the surface species responsible for the reactions observed during the TPD experiments. After the adsorption of 1.1 L of acetaldehyde at 90 K, vibrational modes associated with a multilayer form of acetaldehyde were ob-

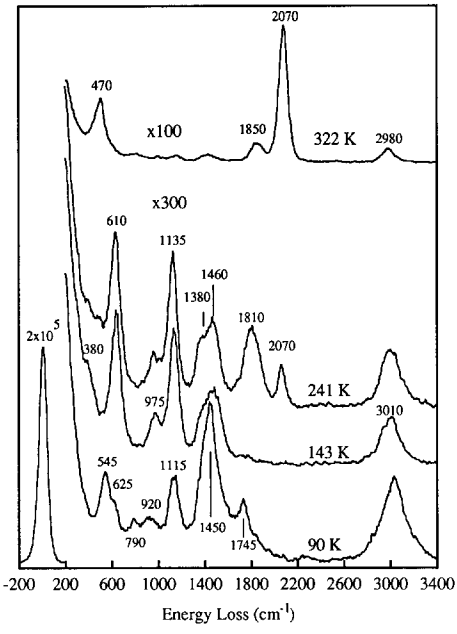

FIG. 5. HREELS after an exposure of 1.1 L of acetaldehyde at 90 K, and HREELS after subsequent heating to 143, 241, and 322 K. An equivalent exposure resulted in the desorption of 0.13 ML of CO.

served. This assignment was based on the identification of a ν(CO) mode at 1745 cm^{-1} in the 90 K spectrum of Fig. 5. The prominent methyl and C—C modes in this spectrum match the IR assignments for crystalline acetaldehyde. The frequencies for crystalline acetaldehyde (*17*) are summarized in Table 2. The methyl modes for the acetaldehyde overlayer were $\nu(CH_3)$ at 3010 cm^{-1}, $\delta(CH_3)$ at 1400 cm^{-1}, and $\rho(CH_3)$ at 920 cm^{-1}. Skeletal modes were also observed, γ(CCO) at 545 cm^{-1} and ν(CC) at 1115 cm^{-1}, and are listed under the multilayer column in Table 2.

Upon heating to 143 K the acetaldehyde overlayer was partially removed and partially converted to an η^2(C,O)-acetaldehyde species on the surface. During TPD experiments acetaldehyde was observed to desorb at 140 K. Acetaldehyde desorption and the change in the adsorbed state were indicated in the sequence of HREEL spectra by the elimination of the vibrational loss peak at 1745 cm^{-1} and the increase in intensity of loss peaks at 610 and 1460 cm^{-1}. The loss at 1460 cm^{-1} in the 143 K spectrum was assigned to the ν(CO) mode of η^2(C,O)-acetaldehyde. Further heating of the surface did not result in any changes in the vibrational modes assigned to acetaldehyde, but modes associated with CO began to appear. Except for the losses assigned to the ν(CO) modes of carbon monoxide (1810 and 2070 cm^{-1}), all vibrational modes in the 241 K spectrum of Fig. 5 were consistent with the presence of an η^2(C,O)-acetaldehyde intermediate bound to the surface. The mode assignments for η^2(C,O)-acetaldehyde are compared to similar modes on Ru(0001) (*7*) and Pd(111) (*8*) in Table 2. The vibrational modes for acetaldehyde on Ru(0001) were taken from the work by Henderson *et al.* (*7*). These workers originally assigned the surface species observed after low doses of acetaldehyde (0.17 L) to a polymeric form. Their conclusions were based on comparison with spectra of species formed after ketene adsorption and on the difficulty of resolving losses in the 1300–1500 cm^{-1} range assignable to the ν(CO) modes of η^2(C,O)-CD_3CDO. In light of subsequent observations for acetaldehyde on Pd(111) (*8*) and Rh(111), we have reassigned their low coverage spectra to an η^2(C,O)-acetaldehyde intermediate. At the low coverage of acetaldehyde examined on Ru(0001) polymerization would be unlikely, and if the C=O bond were roughly parallel to the surface one would not expect it to have strong dipole activity. The assignment of the ν(CO) modes for η^2-acetaldehyde on all these metals is problematic. Since the extents of rehybridization of the C=O bond and of back-bonding to the π^* orbitals are very dependent on the relative orientations of the orbitals of both the carbonyl group and the metal surface, the vibrational frequency of acetaldehyde bonded in the η^2(C,O)-configuration did not show a monotonic trend across the periodic series Ru, Rh, and Pd.

The assignment of the surface species as η^2(C,O)-acetaldehyde was confirmed by

TABLE 2

η^2-Acetaldehyde HREELS Assignments, Frequency (cm^{-1})

Mode	Acetaldehyde					Acetaldehyde-d_4		
	Crystalline[17]	Multilayer	Ru[7]	Rh	Pd[8]	Ru[7]	Rh	Pd[8]
$\nu(CH_3)$	2964/2918	3000	2970	2980	2990	2240	2230	2215
$\nu(C{=}O)$	1722	1745	1395	1460	1390	1380	1440	1400
$\delta(CH_3)$	1431/1389	1450	1340	1380	1390	1030	980	975
$\nu(C{-}C)$	1118	1135	1095	1135	1080	1090	1115	1065
$\rho(CH_3)$	882	920	915	950	930	770	780	800
$\delta(C{-}C{-}O)$	522	545	605	610	600	540	560	550

comparison of the 241 K spectrum of Fig. 5 with a similar spectrum acquired after the adsorption of acetaldehyde-d_4. This comparison is shown in Fig. 6. The 241 K spectrum of Fig. 5 is reproduced with lines connecting the modes to the corresponding modes in the spectrum of the deuterated molecule. The vibrations that involve deformations of the C—H bond shift to lower frequency upon deuterium substitution. The largest shifts were observed for the methyl modes: $\delta(CH_3)$ (1380 to 980 cm^{-1}), $\nu(CH_3)$ (2980 to 2230 cm^{-1}), and $\rho(CH_3)$ (950 to 780 cm^{-1}). The ν(CO) loss shifted only slightly. It was observed as a single peak at 1440 cm^{-1} in the spectrum of η^2(C,O)-CD_3CDO. The absence of another loss in the range of 1400–1600 cm^{-1} indicated that only one kind of carbonyl existed on the surface at this temperature. Davis and Barteau observed two ν(CO) modes in this region at 170 K for acetaldehyde adsorbed on Pd(111) (*8*). Losses at 1400 and 1595 cm^{-1} were assigned to η^2(C,O)-acetaldehyde-d_4 and η^1(C)-acetyl-d_3, respectively, on Pd(111). Thus loss of the aldehyde hydrogen from η^2(C,O)-acetaldehyde and reconfiguration of the bonding resulted in an upward shift in the ν(CO) vibrational frequency of the resulting η^1(C)-acetyl by 195 cm^{-1} on Pd(111). Since this higher frequency ν(CO) vibration was not evident, the acetyl was apparently not formed as a stable, isolable species on Rh(111).

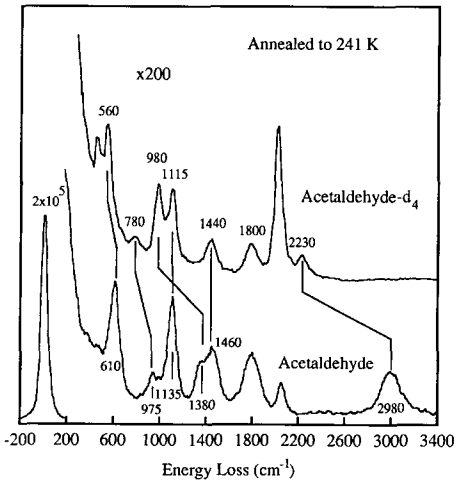

FIG. 6. Comparison of the HREELS after an exposure of 1.1 L of acetaldehyde with the HREELS after an exposure of 1.1 L acetaldehyde-d_4 at 90 K. The surface was annealed to 241 K before taking the spectrum in both cases. An equivalent exposure resulted in the desorption of 0.13 ML of CO for both molecules.

The decarbonylation of the η^2(C,O)-acetaldehyde intermediate occurred between 241 and 322 K. The losses in the 322 K spectrum of Fig. 5 are characteristic of CO adsorbed on the Rh(111) surface. The ν(CO) mode of linearly bonded CO was observed at 2070 cm^{-1} while a small amount of bridge-bonded CO was also indicated by the loss at 1850 cm^{-1}. The loss at 470 cm^{-1} is the ν(*M*-CO) mode of adsorbed CO. The other lower intensity modes in this spectrum are likely due to hydrocarbon fragments on the surface. The ν(C—H) mode of these fragments

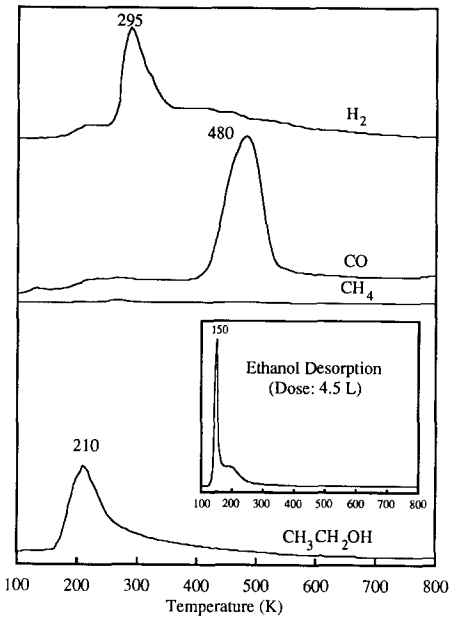

FIG. 7. TPD after an exposure of 1.1 L of ethanol at 90 K. Yields corresponding to this spectrum were 0.47 ML of hydrogen, <0.01 ML of methane, 0.13 ML of surface carbon, 0.14 ML of carbon monoxide, and 0.22 ML of ethanol. After higher exposures an ethanol peak was also observed at 150 K; see inset.

was observed at 2980 cm^{-1}. The TPD spectrum after an acetaldehyde exposure similar to the one used for this HREEL spectrum is illustrated in Fig. 1. The hydrogen TPD peaks are consistent with the HREELS results. Hydrogen was desorbed in a peak exhibiting a maximum at 295 K, and the HREELS indicated that acetaldehyde decarbonylated to produce CO in this temperature range. A higher-temperature hydrogen desorption feature was also observed in TPD at 390 K. This peak was consistent with the dehydrogenation of surface hydrocarbon fragments which were indicated in the HREELS.

Ethanol on Rh(111)

Ethanol decomposed unselectively on the clean Rh(111) surface. Figure 7 shows the TPD spectrum after exposure of the crystal to 1.1 L of ethanol at 90 K. Hydrogen desorbed from the surface over a wide temperature range, from 250 to 600 K. Approximately 50% of the hydrogen was desorbed in a peak exhibiting a maximum at 295 K. This desorption was similar in peak temperature to that observed after exposing the crystal to H_2 to produce a similar hydrogen atom coverage, thus there must have been a reaction that released hydrogen atoms to the surface below this temperature. Due to the broad nature of the hydrogen desorption between 350 and 600 K, it was difficult to identify the surface species responsible for this hydrogen evolution on the basis of its decomposition temperature. However, since the CO desorption peak at 480 K was clearly desorption limited, decarbonylation of surface intermediates must have occurred below 400 K, the onset of the CO desorption. Thus the broad hydrogen desorption between 350 and 600 K was assigned to the dehydrogenation of hydrocarbon fragments on the surface. The complete dehydrogenation of ethanol on the Rh(111) surface was observed for all initial ethanol coverages. Figure 8a is a plot of hydrogen and surface carbon yield versus the yield of carbon monoxide, analogous to the acetaldehyde data of Fig. 3. The slopes of these lines reflected the stoichiometry of ethanol; the only decomposition pathway observed during the TPD experiments was complete dehydrogenation to CO and surface carbon. The spectrum illustrated in Fig. 7 corresponds to an ethanol exposure that resulted in saturation of the decomposition pathway; even at saturation exposures the decomposition of ethanol produced less than 0.01 ML of methane. This can be contrasted to the 50% selectivity to methane observed for acetaldehyde decomposition at similar coverages. Since the decomposition of ethanol would liberate two more hydrogen atoms per methyl group than that of acetaldehyde, and since addition of hydrogen to the surface enhanced methane production during acetaldehyde TPD experiments, one would expect any acetaldehyde formed in the course of ethanol decomposition to exhibit enhanced selectivity to methane. The lack of significant

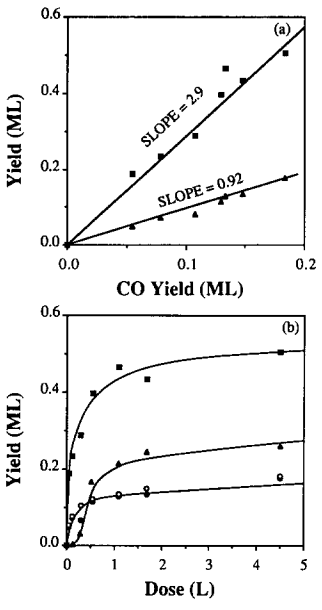

FIG. 8. (a) TPD yields after ethanol exposures (■H_2, ▲ surface carbon) plotted versus the yield of CO. (b) TPD yields after ethanol exposures (■H_2, ○CO, ● surface carbon, ▲ ethanol) plotted versus ethanol exposure.

methane production from ethanol indicates either that the decomposition of ethanol did not proceed via an acetaldehyde intermediate, or that acetaldehyde produced from ethanol was inhibited from decomposing via one of its characteristic pathways.

An additional difference between the behavior of ethanol and acetaldehyde was observed in the desorption of the parent molecules. Ethanol desorbed from the surface in TPD experiments even for initial coverages below those required for saturation of the first layer. For example, after an exposure of 0.29 L approximately 25% of the total adsorbed ethanol desorbed intact; the remainder decomposed to hydrogen, carbon monoxide, and surface carbon. After higher exposures, desorption of the parent molecule rather than decomposition became the dominant mode of ethanol removal from the surface. The relative importance of desorption versus decomposition as a function of ethanol exposure is illustrated in Fig. 8b. For the largest exposure shown, 58% of the ethanol was removed from the first monolayer by desorption. As can be concluded from the hydrogen, carbon monoxide, and surface carbon data in Fig. 8b, the decomposition channel was saturated by 1 L of ethanol exposure. The ethanol coverage shown in this figure was determined by integrating the area of the desorption peak at 200 K. This peak was assigned to the desorption of ethanol bound in the first monolayer. For ethanol exposures greater than 1 L, integration of the 200 K peak required the removal of the large sharp peak at 150 K associated with desorption of ethanol multilayers. An ethanol desorption spectrum exhibiting both the monolayer and multilayer peaks is shown in the inset of Fig. 7. The separation of the parent molecule desorption into these two parts was previously suggested by Sexton *et al.* (*18*). They reported very similar desorption peaks following the adsorption of methanol, ethanol, propanol, and butanol on the Pt(111) surface. The peak temperatures reported for ethanol desorption from that surface were also quite similar to those observed on the Rh(111) surface. Their XPS experiments confirmed that the alcohol molecules adsorbed in the first monolayer were distinct from molecules in the multilayer.

The surface intermediates responsible for the various desorption products were identified by HREELS. The spectra shown in Fig. 9 were obtained after exposing the clean Rh(111) surface to 1.1 L of ethanol at 90 K. The yield versus exposure plot in Fig. 8b indicated that this exposure resulted in saturation of the first monolayer. The 90 K spectrum of Fig. 9 was assigned to molecular ethanol. This assignment was based on the close correspondence between the observed vibrational frequencies of the molecule on the surface and those reported for ethanol in the gas phase (*19*) and in a solid argon matrix (*20*). The original mode assignments of the gas phase spectra distinguished between the C—C and C—O modes. The force constants for the C—C and the C—O bonds are sufficiently similar for these modes to

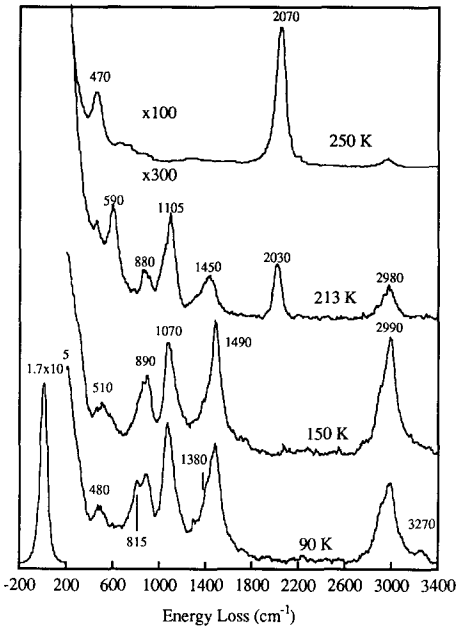

FIG. 9. HREELS after an exposure of 1.1 L of ethanol at 90 K, and HREELS after subsequent heating to 150, 213, and 250 K. An equivalent exposure resulted in the desorption of 0.13 ML of CO in TPD.

combine to give a symmetric and asymmetric doublet; these are reassigned in Table 3 to the combined modes ν_a(CCO) and ν_s(CCO). The other ethanol assignments are also summarized in Table 3. By comparing the frequencies of the modes observed for ethanol on the surface with those in the solid matrix, it was clear that most of the ethanol vibrations were unperturbed by adsorption on the metal surface. The modes associated with the methyl and methylene moieties were $\nu(CH_3)$ at 2990 cm^{-1}, $\delta(CH_2)$ at 1490 cm^{-1}, $\delta(CH_3)$ at 1380 cm^{-1}, and $\gamma(CH_2)$ at 815 cm^{-1}. Each of these modes was at the same frequency as those reported in the solid phase, within the resolution of our experiments. The vibrational frequencies of the C—C—O skeleton were similar to those observed in the reference spectrum. These vibrations were observed at 1070 cm^{-1} for the ν_a(CCO) mode and 890 cm^{-1} for the ν_s(CCO) mode for ethanol on Rh(111). The δ(CCO) mode was observed at a frequency 61 cm^{-1} higher than in the solid phase. This shift was attributed to the steric interactions of the methyl and methylene groups with the surface that restricted the motion of the atoms associated with this mode.

Both the O—H bend and stretch modes were softened on the surface. The ν(OH) mode reported at 3676 cm^{-1} in the solid phase was located at 3270 cm^{-1} on the surface, and the γ(OH) mode at 1241 cm^{-1} shifted to 815 cm^{-1} upon adsorption. Methanol on the Rh(111) surface exhibited similar vibrational frequencies for these modes; the corresponding methanol frequencies were 3230 cm^{-1} for the ν(OH) mode and 825 cm^{-1} for the γ(OH) mode (*21*). The lack of perturbation of the majority of the modes and the softening of the OH modes indicated that ethanol bonded to the surface via its oxygen atom. This bond most likely involved the donation of lone pair electrons on the oxygen to the surface. Similar bonds are formed between other oxygenates and metal surfaces. For example, Walczak *et al.* (*22*) compared the adsorption and desorption of perfluorodiethyl ether and hexafluoroacetone on the Ru(0001) surface with those of their fully hydrogenated analogs. They concluded that these molecules bonded via electron donation to the surface, since the fluorinated molecules were more weakly bound. Fluorination inductively reduced the availability of the lone pair electrons of the oxygen and thus reduced the surface-adsorbate bond strength.

HREEL spectra were also collected after the adsorption of ethanol-d_6. These spectra are illustrated in Fig. 10. The 90 K spectrum of this figure was assigned to molecular ethanol. The ν(OD) mode was observed at 2400 cm^{-1}. The H/D frequency ratio of this mode was 1.36 which indicated that the shift was due solely to the deuterium substitution. The $\nu(CD_3)$ and $\nu(CD_2)$ modes were found at 2240 and 2110 cm^{-1} as expected. However, the assignment of the other bands was complicated by the strong coupling of the methyl and methylene deformation modes with the C—C—O stretching modes. Since

TABLE 3

Ethanol HREELS Assignments, Frequency (cm^{-1})

Mode	Ethanol			Ethanol-d_6	
	Gas[19]	Solid[20]	Rh(90 K)	Gas[19]	Rh(90 K)
ν(OH)	3660	3676	3270	2710	2400
$\nu(CH_3)$	2965/2880	2989/2943	2990	2240/2100	2240
$\nu(CH_2)$	—	2900	nr	—	2110
$\delta(CH_2)$	1450	1490	1490	1160	1145
$\delta(CH_3)$	1390	1452/1394	1380	1060	1090
γ(OH)	—	1241	815	—	560
ν_a(C—C—O)	1060	1089	1070	970	970
$\rho(CH_3)$	—	1033	nr	—	nr
ν_s(C—C—O)	880	885	890	800	750
$\gamma(CH_2)$	—	801	815	—	560
δ(C—C—O)	—	419	480	—	450

Note. nr, not resolved.

the ν_a(CCO) and ν_s(CCO) vibrations were no longer distinct from the C—D vibrations, the frequencies assigned to these modes differed significantly from the corresponding frequencies observed after ethanol adsorption. In the case of ethanol-d_6, the assignment of vibrations to the ν_a(CCO), ν_s(CCO), $\delta(CD_3)$, and $\delta(CD_2)$ modes is a somewhat artificial construction, since all normal modes in the 750 to 1145 cm^{-1} range involve motions of all eight of these atoms. The assignments listed in Table 3 are consistent with reference spectra but should only be considered as approximate.

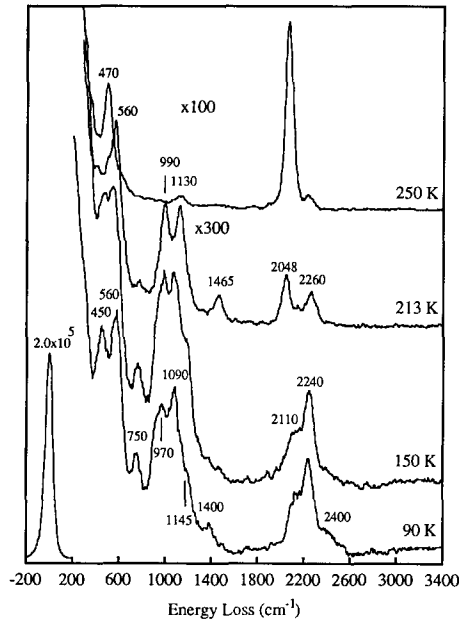

FIG. 10. HREELS after an exposure of 1.1 L of ethanol-d_6 at 90 K, and HREELS after subsequent heating to 150, 213, and 250 K. An equivalent exposure resulted in the desorption of 0.13 ML of CO in TPD.

Upon heating the Rh(111) surface to 150 K both ethanol and ethanol-d_6 dissociated to form the respective ethoxides. The vibrational spectra of the ethoxides were very similar to the spectra of the parent alcohols. The mode assignments are summarized in Table 4. The ν(OH) mode at 3270 cm^{-1} and the γ(OH) at 815 cm^{-1} were eliminated by heating the surface to 150 K as illustrated by the comparison of the 150 K and the 90 K spectra of Fig. 9. Similar reductions in intensity in the O—D modes at 2400 and 560 cm^{-1} were observed for the deuterated case. After heating the surface to 213 K several reactions were evident. The appearance of a peak at 1465 cm^{-1} in the 213 K spectrum of Fig. 10 provided evidence for the production of a small amount of η^2(C,O)-acetaldehyde-d_4. If 50% of any acetaldehyde formed from ethoxide dehydrogenation is assumed to decarbonylate to give methane, then the methane yield of the TPD experiment illus-

TABLE 4

Ethoxide HREELS Assignments, Frequency (cm^{-1})

Mode	Ethoxide			Ethoxide-d_5		
	Rh	Pd[10]	Cu[19]	Rh	Pd[10]	Cu[19]
$\nu(CH_3)$, $\nu(CH_2)$	2990	2925	2970/2860	2240/2110	2230/2100	2240/2090
$\delta(CH_2)$	1405	1465	1450	1130	1070	1170
$\delta(CH_3)$	1390	1400	1380	1090	1070	1070
ν_a(C—C—O)	1070	1040	1030	970	960	980
ν_s(C—C—O)	880	855	870	750	740	760
$\gamma(CH_2)$	nr	745	—	560	560	—
δ(C—C—O)	510	450	470	450	440	430
ν(M—O)	nr	—	270	nr	—	270

Note. nr, not resolved.

trated in Fig. 7 indicated that less than 10% of the ethoxide decomposed via an acetaldehyde intermediate.

A comparison of the spectrum obtained after acetaldehyde adsorption and the 213 K spectrum of Fig. 9 is illustrated in Fig. 11. Although the ethanol spectrum of Fig. 11 was very similar to the acetaldehyde spectrum, most of the intensity could be attributed to ethoxide vibrations. The significant downward shift of all the ethanol modes relative to the acetaldehyde spectrum and the absence of a 975 cm^{-1} loss in the ethanol spectrum support the assignment as ethoxide rather than acetaldehyde. In parallel with the minor dehydrogenation that produced acetaldehyde was the principal reaction to yield carbon monoxide. η^2(C,O)-Acetaldehyde formed by acetaldehyde adsorption on the Rh(111) surface did not begin to decompose until 240 K. Heating the acetaldehyde-dosed surface to 213 K did not result in any significant formation of carbon monoxide, as shown in Fig. 11, but heating the ethanol-dosed surface to 213 K produced adsorbed carbon monoxide, fingerprinted by the losses at 470 and 2030 cm^{-1}. Thus another pathway for ethanol decomposition must exist in parallel with that leading to acetaldehyde. Comparison of the 250 K spectrum of Fig. 9 and the 241 K spectrum of Fig. 5 showed a striking difference. The decomposition of surface species formed from ethanol was complete by 250 K; vibrational modes associated with carbon monoxide dominated the 250 K spectrum of the adlayer formed from ethanol but not acetaldehyde. Thus ethoxide decomposed completely at a lower temperature than did acetaldehyde. Another difference between the ca. 250 K spectra of the ethanol and acetaldehyde-derived adlayers was the binding

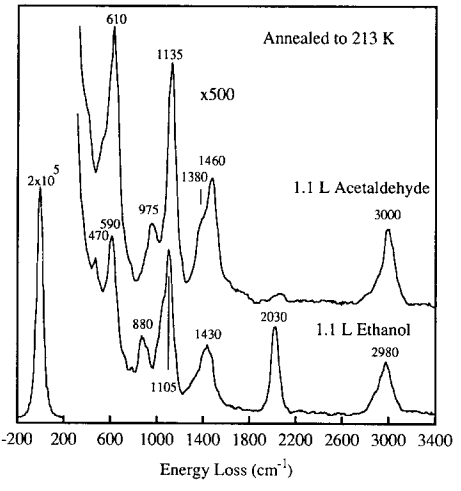

FIG. 11. Comparison of the 213 K spectrum of Fig. 9 with the HREEL spectrum obtained after an exposure of 1.1 L of acetaldehyde and annealing to 213 K. The scales of these spectra have been adjusted to be the same.

site of the CO. In the case of acetaldehyde, the majority of the carbon monoxide was bound in the bridge-bonded state, as indicated by the loss at 1810 cm^{-1}. In contrast, carbon monoxide formed from ethanol decomposition bonded exclusively in the linear state, with a vibrational frequency of 2070 cm^{-1}.

In summary, there were several differences between the behavior of ethanol and acetaldehyde on the Rh(111) surface that indicated the existence of nonintersecting decomposition pathways for these two molecules. One example was the fate of the methyl groups of ethanol and acetaldehyde. Acetaldehyde decomposition after an exposure that saturated the first layer resulted in 50% methane and 50% carbon deposition while ethanol decomposition resulted essentially in only carbon deposition. The thermal stability of ethanol was lower than acetaldehyde. All oxygen-containing surface intermediates formed from ethanol had decomposed to carbon monoxide by 250 K as shown by HREELS, but η^2(C,O)-acetaldehyde was still the dominant intermediate at 241 K following acetaldehyde adsorption. Finally, acetaldehyde did appear to be a minor decomposition intermediate of ethanol, but the major decomposition pathway was via dehydrogenation of an ethoxide intermediate that did not proceed via acetaldehyde.

DISCUSSION

Acetaldehyde exhibited 50% selectivity to methane during decomposition on the Rh(111) surface. This product resulted from the reaction of atomic hydrogen with methyl groups eliminated from acetaldehyde. The mechanism of this methyl elimination was likely similar to the alkyl migration reaction widely reported to occur on transition metal complexes. On Rh complexes, decarbonylation of acyls via methyl migration has been shown to be thermodynamically and kinetically favorable at moderate temperatures in the absence of CO (*23, 24*). Conversely, at elevated pressures of CO, alkyl migration to CO is the critical step in the homogeneous "oxo" process used to produce linear aldehydes from olefins and carbon monoxide, and in the Monsanto acetic acid process for methanol carbonylation. Both of these processes use Rh complexes as catalysts. Ethylene hydroformylation on supported Rh/SiO_2 has recently been reported by Chuang and Pien (*25*). They provide *in situ* IR evidence for acyl intermediates and suggest that these are formed by alkyl migration. The large number of examples of alkyl migration on mononuclear complexes, including those of rhodium, does not necessarily imply that this pathway is operative on surfaces; however, it is the most plausible candidate to explain our observations for acetaldehyde decarbonylation on Rh(111). In their attempt to extend the cluster-surface analogy (*26*), Blyholder and Lawless have recently used semiempirical molecular orbital calculations to explore the relationship between formyl formation occurring on organometallic mononuclear complexes and on small clusters of metal atoms (*27*). Their calculations indicated that the large number of orbitals in the valence band of the metal cluster permitted many bonding structures of similar energies, whereas the mononuclear complex had only a few orbitals available, limiting it to a few stable structures. Thus reactions that occur on mononuclear complexes would be expected to be a subset of those feasible on surfaces. There do, however, appear to be differences between the ligands on mononuclear complexes and intermediates formed on surfaces. For example, the formation of stable η^1(C)-acetyls, common for Rh complexes, was not observed on the Rh(111) surface; acetaldehyde coordinated in the η^2(C,O)-configuration. We regard acetyls as likely transient intermediates in the decarbonylation of acetaldehyde on Rh(111), given the otherwise close parallel between the surface and the cluster chemistry and the appreciable activity of the surface for a variety of dehydrogenation reactions.

The dehydrogenation activity of Rh(111) was clearly evident in the decomposition of

ethanol; dehydrogenation of this molecule was complete and unselective. The first step was the formation of an ethoxide which was complete by 150 K. Alkoxides have been widely observed as intermediates in alcohol decomposition sequences (*9, 10, 19, 21*). The ethoxide intermediate then dehydrogenates at either the methylene or methyl position. Loss of hydrogen from the methylene group would result in the formation of an aldehyde intermediate. Loss of this hydrogen has been reported to be the primary mode of ethoxide decomposition on Pd(111) (*10*) and Ni(111) (*11*). This pathway appeared to be a minor one for ethoxides on Rh(111); the principal channel for ethoxide dehydrogenation on this surface did not appear to involve adsorbed acetaldehyde. This conclusion was supported by the absence of methane desorption after ethanol adsorption, and the assignment of the majority of the losses in the HREEL spectra to ethoxides. These observations suggest that ethoxide dehydrogenation occurs primarily via cleavage of a C—H bond on the methyl group. Loss of hydrogen at the methyl position of the ethoxide would result in the formation of an oxametallacycle intermediate that would be difficult to characterize even if it were stable, since its skeletal bonds would be roughly parallel to the surface and thus not dipole active. The point at which C—C bond scission occurs in the ethoxide dehydrogenation sequence is not clear, but this scission must occur before complete dehydrogenation of the C—C framework, since carbon monoxide bands were evident in the HREEL spectra by 250 K, but evolution of reaction-limited hydrogen from surface hydrocarbon moieties continued until 600 K.

It is striking, not only that the decarbonylation pathways of ethanol and acetaldehyde differ so strongly from each other on Rh(111), but that the chemistry of these molecules also differs significantly on the neighboring metal Pd. Davis and Barteau (*10*) have shown that adsorbed acetaldehyde was formed in high selectivity from ethoxides on the Pd(111) surface. They proposed that the sequence of dehydrogenations: ethanol–ethoxide–acetaldehyde–acetyl–carbon monoxide plus methylene is the single reaction network connecting the oxygenated intermediates on Pd(111). Clearly this reaction network is not the only pathway active for ethanol decomposition on the Rh(111) surface. Even when this network is entered at the acetaldehyde intermediate, Rh does not follow the Pd dehydrogenation sequence. Davis and Barteau (*8*) reported that acetaldehyde or acetyl decomposition on Pd(111) proceeded via removal of a hydrogen from the methyl group followed by C—C bond scission. The reverse of this reaction, methylene migration to carbon monoxide, has been proposed as a mechanism of acetaldehyde formation on Fischer–Tropsch catalysts by Hackenbruch *et al.* (*28*). They support this mechanism with an example of methylene migration observed for a binuclear iron complex. Unstable ketene also may be one of intermediates formed on the Pd surface. Radloff *et al.* (*29*) and Mitchell *et al.* (*30*) have characterized the reactions of ketene on the Pt(111) surface using HREELS and TPD. They observed that the decomposition products of ketene were hydrogenated to methane at higher ketene exposures. Davis and Barteau (*8*) have also observed that the coordination of the vinyl group of acrolein resulted in a decomposition temperature lower than that of the saturated analog, propionaldehyde. Thus the decarbonylation of aldehydes on Pd(111) apparently requires an unsaturated carbon center, while the decarbonylation of acetaldehyde on Rh(111) proceeds via methyl migration.

The results of this study demonstrate that the principal pathways for decomposition of ethanol and acetaldehyde on Rh(111) do not intersect, as illustrated schematically in Fig. 12. This figure depicts to scale the stable and postulated adsorbates encountered along the nonintersecting pathways for decarbonylation of acetaldehyde and ethanol on Rh(111). On a flat open structure such as

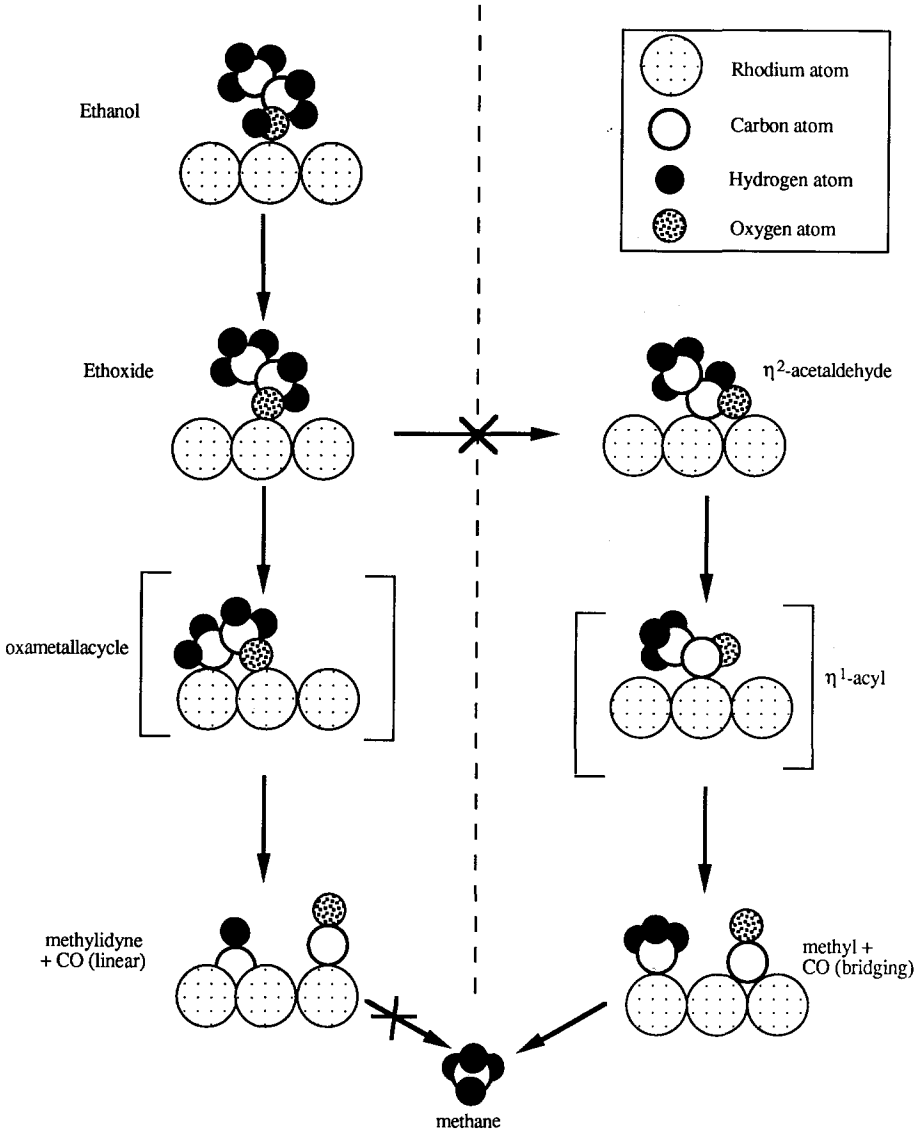

FIG. 12. Reaction sequences observed and [postulated] intermediates in the nonintersecting decarbonylation of acetaldehyde and ethanol on Rh(111).

(111) surface of FCC metals it is difficult to envision significant steric origins of the different decarbonylation pathways for the two molecules. As is clear from Fig. 12, all hydrogens in the adsorbed molecules and the observed ethoxide and η^2-acetaldehyde species have reasonable access to neighboring surface metal atoms. Moreover, one could not explain the dramatic difference in the surface chemistry of these C_2 oxygenates between Rh(111) and Pd(111) surfaces, since the lattice constants of these two metals differ by only about 2%.

While the origin of the nonintersecting decarbonylation pathways for ethanol and acetaldehyde on Rh(111) is unclear, our observations are consistent with isotopic mixing results on catalysts consisting of Rh on non-

interacting supports which showed that ethanol was not formed by sequential hydrogenation of acetaldehyde. In the present study ethoxide intermediates were isolated in the ethanol decomposition sequence and η^2(C,O)-acetaldehyde was the principal form of acetaldehyde. However, more highly dehydrogenated species, such as the ketene intermediate proposed by Takeuchi and Katzer (*1*), could not be isolated. Since there were no oxygen atoms available from a support for carboxylate formation, there was no evidence for the mechanism proposed by Orita *et al.* (*2*). Finally, approximately 10% of the ethanol appeared to dehydrogenate via adsorbed acetaldehyde. This indicated that the hydrogenation/dehydrogenation pathway between acetaldehyde and ethanol was not excluded on the Rh(111) surface, consistent with the results of Underwood and Bell (*4*). Since several of the mechanisms proposed on the basis of experiments with supported catalysts appeared to operate on the Rh(111) surface, the dramatic effect of support interactions on the performance of these catalysts is not surprising. Selection of the preferred channel for the catalytic reaction is likely determined by the modification of the stability of the various intermediates by the support or by promoter atoms on the metallic surface. Thus some caution must be exercised when attempting to extend mechanistic conclusions from one supported rhodium catalyst to another, especially on different supports.

CONCLUSIONS

Ethanol and acetaldehyde do not decarbonylate via a common pathway on Rh(111). Decarbonylation of acetaldehyde, bound to the surface in an η^2-configuration, proceeds via methyl elimination. One-half of the methyl groups produced at saturation coverages are hydrogenated to methane. Ethanol decarbonylation proceeds via the formation of surface ethoxides. These decompose at lower temperatures than does η^2-acetaldehyde, they do not appear to form η^2-acetaldehyde on the surface, and little methane is desorbed. The divergence of ethanol and acetaldehyde decomposition pathways suggests that C—H scission at the methyl position may precede C—C scission in ethoxide decarbonylation. The additional differences in the reaction pathways of C_2-oxygenates on Rh(111) and Pd(111) surfaces suggest that caution must be exercised in attempting to apply a common network for oxygenate synthesis and decomposition on Group VIII metals.

ACKNOWLEDGMENTS

We gratefully acknowledge the support of this research by the Department of Energy, Office of Basic Energy Sciences, Division of Chemical Sciences (Grant FG02-84ER13290). Thanks are due to Nicole Brown for preparing graphics of the reaction network.

REFERENCES

1. Takeuchi, A., and Katzer, J. R., *J. Phys. Chem.* **86,** 2438 (1982).
2. Orita, H., Naito, S., and Tamaru, K., *J. Catal.* **90,** 183 (1984).
3. Jackson, S. D., Brandreth, B. J., and Winstanly, D., *J. Catal.* **106,** 464 (1987).
4. Underwood, R. P., and Bell, A. T., *Appl. Catal.* **21,** 157 (1986).
5. Ichikawa, M., *Bull. Chem. Soc. Jpn.* **51,** 2273 (1978).
6. Lavalley, J. C., Saussey, J., Lamotte, J., Breault, R., Hindermann, J. P., and Kiennemann, A., *J. Phys. Chem.* **94,** 5941 (1990).
7. Henderson, M. A., Zhou, Y., and White, J. M., *J. Am. Chem. Soc.* **111,** 1185 (1989).
8. Davis, J. L., and Barteau, M. A., *J. Am. Chem. Soc.* **111,** 1782 (1989).
9. Davis, J. L., and Barteau, M. A., *Surf. Sci.* **187,** 387 (1987).
10. Davis, J. L., and Barteau, M. A., *Surf. Sci.* **235,** 235 (1990).
11. Gates, S. M., Russell, J. N. and Yates, J. T., Jr., *Surf. Sci.* **171,** 111 (1986).
12. Davis, J. L., and Barteau, M. A., *Surf. Sci.* **208,** 383 (1989).
13. Bent, B. E., Mate, C. M., Crowell, J. E., Koel, B. E., and Somorjai, G. A., *J. Phys. Chem.* **91,** 1493 (1987).
14. Ceyer, S. T., *Ann. Rev. Phys. Chem.* **39,** 479 (1988).
15. Redhead, P. A., *Vacuum* **12,** 203 (1962).
16. Houtman, C. J., and Barteau, M. A., *J. Phys. Chem.* **95,** 3755 (1991).

17. Hollenstein, H., and Gunthard, H. H., *Spectrochim. Acta Part A* **27,** 2027 (1971).
18. Sexton, B. A., Rendulic, K. D., and Hughes, A. E., *Surf. Sci.* **121,** 181 (1982).
19. Sexton, B. A., *Surf. Sci.* **88,** 299 (1979).
20. Barnes, A. J., and Hallam, H. E., *Trans. Faraday Soc.* **66,** 1960 (1984).
21. Houtman, C., and Barteau, M. A., *Langmuir* **6,** 1558 (1990).
22. Walczak, M. M., Leavitt, P. K., and Thiel, P. A., *J. Am. Chem. Soc.* **109,** 5621 (1987).
23. Slack, D. S., Egglestone, D. L., and Baird, M. C., *J. Organomet. Chem.* **146,** 71 (1978).
24. Milstein, D., *Organometallics* **1,** 1549 (1982).
25. Chuang, S. S. C., and Pien, S-I., *J. Mol. Catal.* **55,** 12 (1989).
26. Yang, H., and Whitten, J. L., *J. Chem. Phys.* **91,** 126 (1989).
27. Blyholder, G., and Lawless, M., *J. Am. Chem. Soc.* **111,** 1275 (1989).
28. Hackenbruch, J. Keim, W., Röper, M., and Strutz, H., *J. Mol. Catal.* **26,** 129 (1984).
29. Radloff, P. L., Mitchell, G. E., Greenlief, C. M., Henderson, M. A., White, J. M., and Mims, C. A., *Surf. Sci.* **183,** 377 (1987).
30. Mitchell, G. E., Radloff, P. L., Greenlief, C. M., Henderson, M. A., and White, J. M., *Surf. Sci.* **183,** 403 (1987).